THE DEVELOPMENT OF A METHOD AND APPARATUS TO DETECT LAP AND BUTT WELDS IN A MOVING STEEL STRIP

by

Homer P. Halsey

Submitted in Partial Fulfillment of the Requirements

for the Degree of

Master of Science in Engineering

in the

Electrical Engineering

Program

S. J. Skarote — August 15, 1972
Adviser — Date

Carl E. Kiel — August 15, 1972
Dean of the Graduate School — Date

YOUNGSTOWN STATE UNIVERSITY

August, 1972

ABSTRACT

THE DEVELOPMENT OF A METHOD AND APPARATUS TO DETECT LAP AND BUTT WELDS IN A MOVING STEEL STRIP

Homer P. Halsey

Master of Science in Engineering

Youngstown State University, 1972

The first objective of this investigation was to determine the physical differences between the weld and the base metal. The physical differences were used to create amplitude differences in the retained fields of the magnetized weld and the magnetized base metal.

The difference in mechanical hardness between the weld and base metal was the distinguishing characteristic of the butt welded samples. This property was related to the retained fields and experimentally verified. The difference in thickness between the weld and base metal was the outstanding property of the lap welded samples. This property was also related to the retained fields and was experimentally verified.

The second objective of this investigation was to test several different sensing devices. Some of the devices were specially constructed, while others were purchased. All sensors were tested in the laboratory on a rotating disk with a butt weld through the center. All the devices were evaluated and the sensor that had the best characteristics was selected to be used for the experimental weld detector.

The third objective was to design and construct an experimental weld detector. The circuit for the detector was designed and constructed to compensate automatically for different velocities of the welded strip. The compensation was for frequency and amplitude changes of the sensor signal due to different velocities.

The last objective was to test the detector and to evaluate the basic concepts and experimental results of this investigation. The fields of the magnetized welds of all the samples tested were related to the hardness and thickness of the welds. All the welds tested exhibited the predicted characteristics needed for detection. Before this method could be considered reliable enough for a permanent mill installation many more welds should be tested in the laboratory.

The test results of the experimental weld detector were very encouraging. The detector compensated very well for amplitude and frequency changes of the sensor signal due to velocity changes.

In conclusion, if after testing many more weld samples, it is found that all of them exhibit the required characteristics, then a weld detector, based on the findings of this investigation, is definitely feasible.

ACKNOWLEDGEMENT

I would like to express my gratitude to my adviser, Professor Samual J. Skarote, for his constructive criticisms, and for his help in constructing the experimental weld detector. I would also like to thank Dr. Matthew Siman and Professor Raymond E. Kramer for their helpful suggestions.

TABLE OF CONTENTS

LIST OF SYMBOLS

SYMBOL	DEFINITION	UNITS OR REFERENCE
e_i	Input Voltage	Volts
e_o	Output Voltage	Volts
J	Operator	$\sqrt{-1}$
x	Distance	cm
t	Time	Seconds
A	Area	cm^2
A_1	Voltage Gain	Volt/Volt
A_2	Voltage Gain	Volt/Volt
B	Flux Density	Gauss
C	Capacitance	Farads
I	Current	Amperes
K	Constant	See eqs. (1),(3),(9)
K_1	Constant	See eq. (37)
K_2	Constant	See eq. (38)
K_3	Constant	See eq. (44)
K_4	Constant	See eq. (45)
N	Turns	
R	Resistance	Ohms
S	Differential Operator	Laplace Variable
T	Period	Sec./Cycle
V	Velocity	cm./sec.
W	Angular Frequency	Radians/Sec.
ø	Flux	Maxwells
θ	Angle	Degrees

LIST OF FIGURES

LIST OF FIGURES

LIST OF FIGURES

- - - - - - - - - - - - -

INTRODUCTION

The purpose of this investigation is to develop a noncontact, nondestructive method and apparatus to detect welds in a continuously moving steel strip.

Welds need to be detected and removed to prevent damage to costly dies and other equipment of the steel producer's customers. Butt welds are harder than the strip and may break or mark a die. Lap welds are thicker than the strip and may also damage the die or jam some of the processing equipment.

Also, the product made from a strip containing a weld may be inferior since a butt weld will often crack or break and a lap weld may partially open. Then it may be necessary to reject the product that contains the weld. Therefore, good, reliable, low maintenance weld detectors are needed not only in steel plants, but also in fabricating plants.

At present, the location of a weld is determined by using a light source and photoelectric cell to find a hole which is punched adjacent to the weld at the time the weld is made.

This system of locating welds has several major problems. The hole punching mechanism requires considerable maintenance to keep the system functioning properly. The hole detecting mechanism not only requires considerable

maintenance, but also presents problems in eliminating ambient light to avoid false weld indication signals.

The weld detection method used in this study is related to the amplitude differences of the retained fields of the magnetized weld and the magnetized base metal. The physical contrasts cause differences in the retained fields of the magnetized weld and magnetized base metal. The difference of retained fields is sensed by either Hall devices or inductive pickups which develop a voltage that is a function of the field differences. The voltage is then processed by the weld detector circuitry to produce an output signal which indicates the presence of the weld. An experimental laboratory weld detector was designed, built, tested, and evaluated in this study.

CHAPTER I

RELATING PHYSICAL DIFFERENCES OF WELDS AND BASE METAL TO DIFFERENCES IN RETAINED FIELDS

In order to develop a method and apparatus to detect lap and butt welds in a moving steel strip, it was necessary to determine differences in the weld and base metal.

In order to determine these differences, samples of lap and butt welds were collected and tests were run on these samples. Figures 1 and 2 below are edge views of lap and butt welds. These tests involved cutting small samples

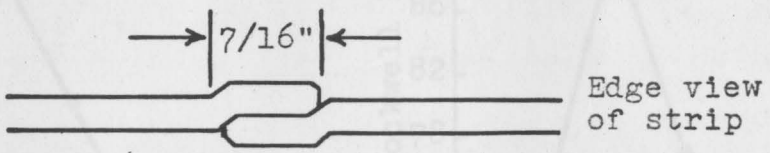

Figure 1. Lap Weld

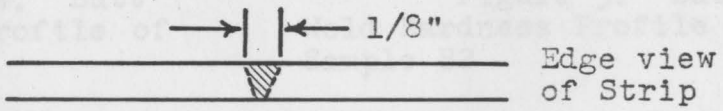

Figure 2. Butt Weld

from the larger samples. The small samples were about two inches long and a half inch wide. The weld area was one inch from each end of the sample. Using a Rockwell hardness tester, the mechanical hardness was measured at the center of the weld and at one-quarter inch and one-half inch, respectively, on either side of the weld.

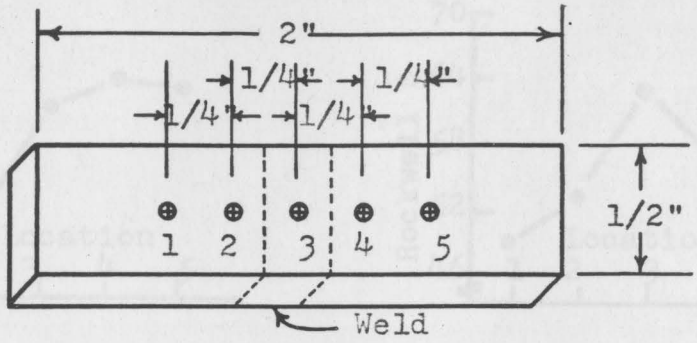

Figure 3. Rockwell Measurement Locations

The hardness profile of butt welds indicated there are differences in mechanical hardness between the weld and the base metal. The hardness profile of lap welds did not

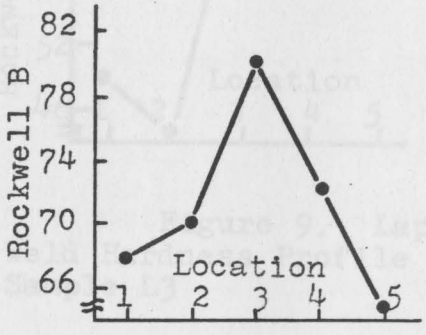

Figure 4. Butt Weld Hardness Profile of Sample B1

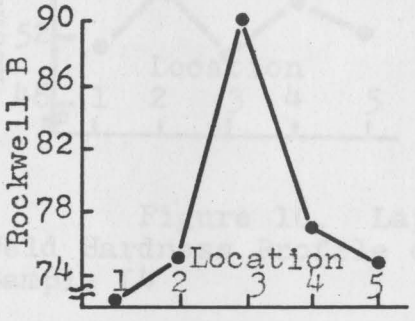

Figure 5. Butt Weld Hardness Profile of Sample B2

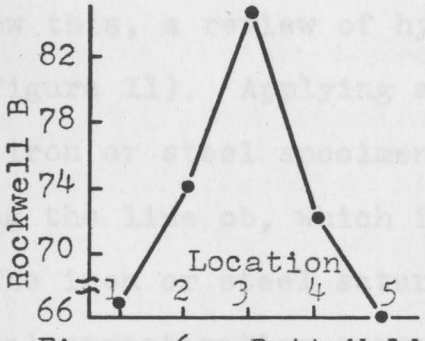

Figure 6. Butt Weld Hardness Profile of Sample B3

indicate a large difference in mechanical hardness between the lap weld and the base metal. The physical characteristic of the lap weld is that it is thicker than the base metal.

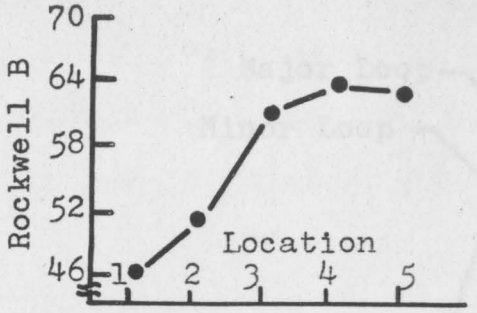

Figure 7. Lap Weld Hardness Profile of Sample L1

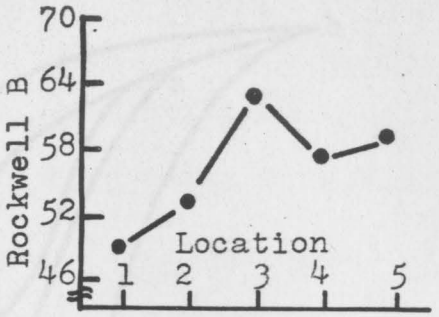

Figure 8. Lap Weld Hardness Profile of Sample L2

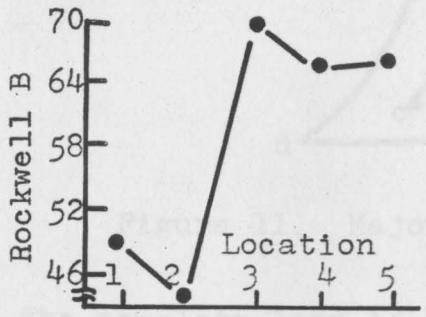

Figure 9. Lap Weld Hardness Profile of Sample L3

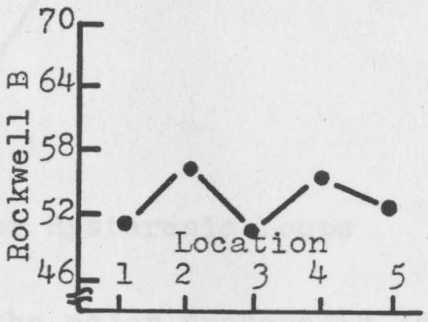

Figure 10. Lap Weld Hardness Profile of Sample L4

Both hardness and thickness can be related to the retained field.

To show this, a review of hysteresis loops will be helpful (see Figure 11). Applying an increasing magnetic field H to an iron or steel specimen increases the flux density B along the line ob, which is the normal magnetization curve. The iron or steel saturates at the point at which the normal magnetization curve becomes a straight line. As H is decreased, B does not retrace its path, but travels the path bB_{rs}. When H is reversed, B follows the path $B_{rs}H_{cs}d$ and the loop closes on itself when H is returned to "b."

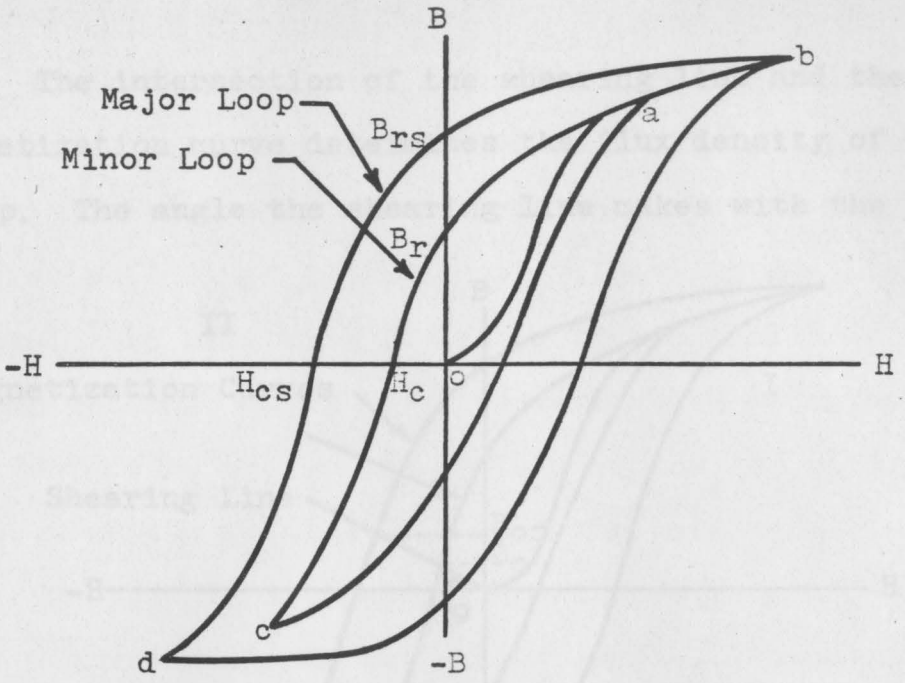

Figure 11. Major and Minor Hysteresis Loops

The complete loop is known as the major hysteresis loop of the particular specimen under test. If the same material were initially magnetized to "a" rather than "b" and H is reversed, B follows the path $B_r H_c c$, and the loop closes on itself when H is returned to "a." This complete loop is known as a minor hysteresis loop.

The second quadrant of the hysteresis loop is of primary concern. This second quadrant curve is called the demagnetization curve. The intersection of the demagnetization curve with the horizontal axis gives the coercive force H_c. The coercive force H_c and the mechanical hardness of iron or steel decrease as impurity content decreases, as internal strains are removed, and as grain size increases. Therefore, a measurement that is related to the coercive force should also be related to the hardness.

The intersection of the shearing line and the demagnetization curve determines the flux density of the air gap. The angle the shearing line makes with the

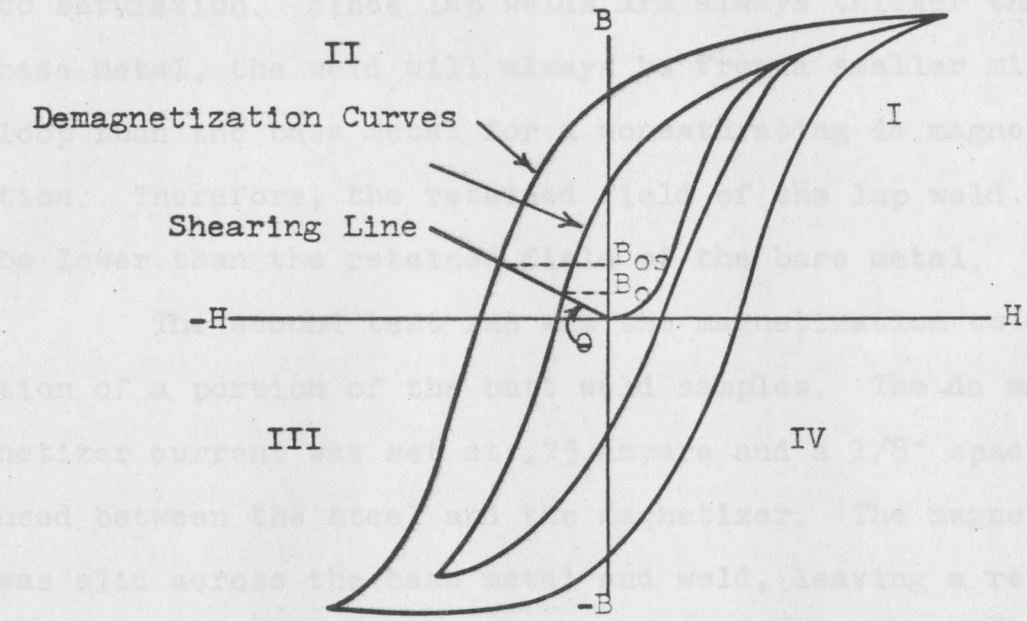

Figure 12. Shearing Line on Demagnetization Curves

horizontal axis is:

$$\theta = \tan^{-1} L_m/KL_g \qquad (1)$$

where L_m = length of the magnet, L_g = length of the gap, and K = a constant which is much greater than one. If a large air gap is employed, θ is very small and:

$$B_{os} \approx H_{cs} \tan \theta. \qquad (2)$$

Since tan θ does not change, B_{os} is proportional to H_{cs}. Since H_{cs} is related to mechanical hardness, then B_{os} must also be related to mechanical hardness. Since butt welds exhibit differences in hardness between the weld and the base metal, there should also be differences in the retained fields of the weld and base metal.

To get a relationship that is a function of thickness, demagnetizing curves must be from minor hysteresis loops. This means that the material must not be magnetized to saturation. Since lap welds are always thicker than the base metal, the weld will always be from a smaller minor loop than the base metal for a nonsaturating dc magnetization. Therefore, the retained field of the lap weld should be lower than the retained field of the base metal.

The second test run was the magnetization to saturation of a portion of the butt weld samples. The dc magnetizer current was set at .75 ampere and a 1/8" spacer was used between the steel and the magnetizer. The magnetizer[1] was slid across the base metal and weld, leaving a retained field in the sample. The retained fields were then measured by a Hall probe and gaussmeter. Plots of the data are shown in Figures 14, 15, and 16. The plots illustrate that there are large differences in the retained fields of the welds and the base metal.

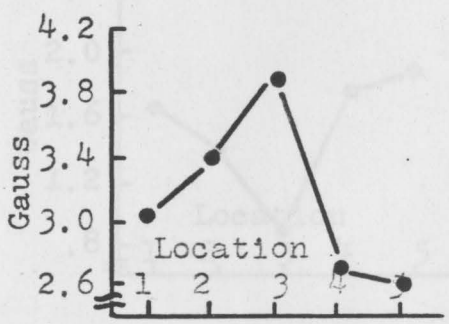

Figure 14. Retained Field Profile of Sample B1

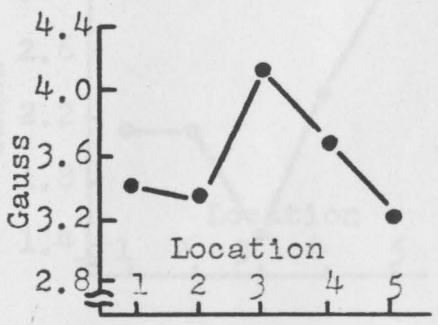

Figure 15. Retained Field Profile of Sample B2

[1]Figure 13, "Magnetizer," is contained in the Appendix.

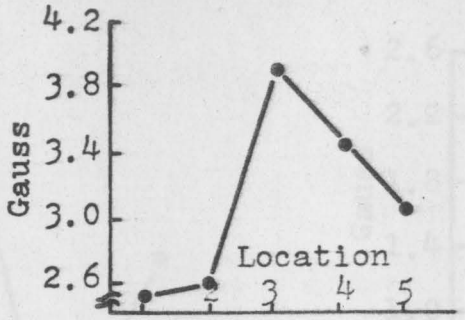

Figure 16. Retained Field Profile of Sample B3

The magnetization of the lap welds and their associated base metal was not to saturation, but was high enough to have as large a retained field as practical. The magnetizer current was set at .25 ampere and a 1/4" spacer was used between the steel and the magnetizer. As in the saturation tests, the magnetizer was slid across the base metal and weld, leaving a retained field in the sample. Again, the retained fields were measured by a Hall probe and gaussmeter. As had been predicted, the retained field of the weld was lower than the base metal.

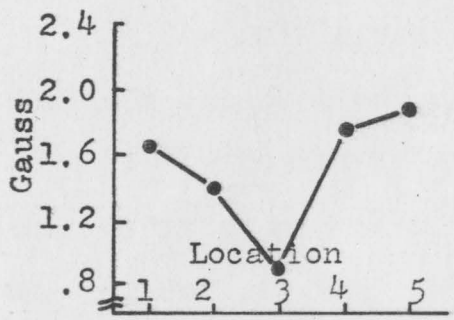

Figure 17. Retained Field Profile of Sample L1

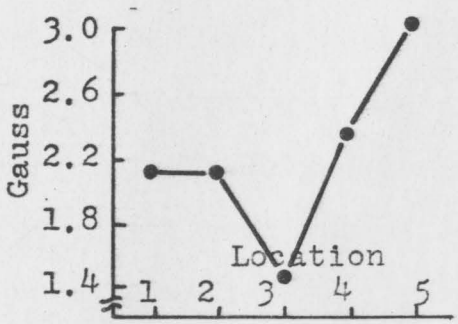

Figure 18. Retained Field Profile of Sample L2

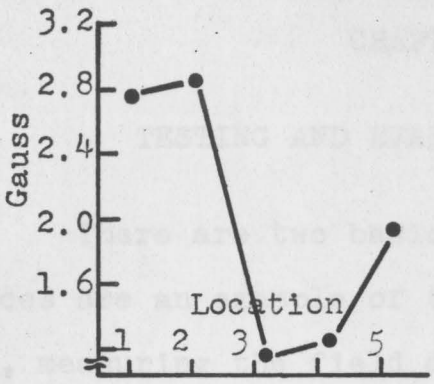

Figure 19. Retained Field Profile of Sample L3

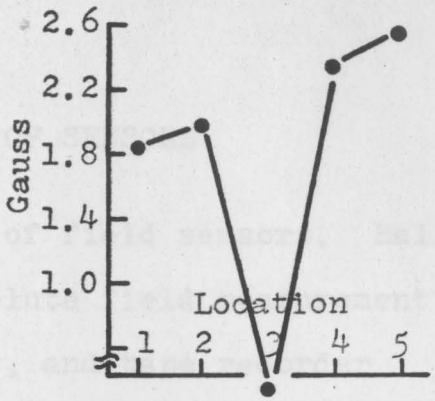

Figure 20. Retained Field Profile of Sample L4

The tests have shown that if the described magnetization is used, the weld and the base metal will exhibit different retained fields. This is true for both butt and lap welds.

CHAPTER II

TESTING AND EVALUATION OF SENSORS

There are two basic types of field sensors. Hall devices are an example of the absolute field measurement type, measuring the field directly, and tape recorder heads are an example of the inductive type, measuring the rate of change of the field.

The potential developed by a single Hall element is

$$e = KIB. \qquad (3)$$

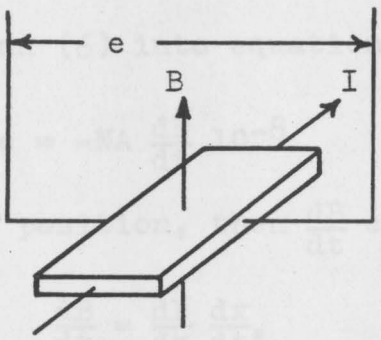

Figure 21. Enlarged Sketch of a Hall Element

The Hall effect is the development of a potential gradient across a current-carrying conductor or semiconductor situated in a magnetic field. The direction of the potential gradient is normal to the directions of both the current and the component of the magnetic field perpendicular to the current.

The differential probe consists of two Hall elements positioned side by side. The elements are electrically connected to subtract one voltage from the other. If they sense equal fields, they develop equal voltages and there is

no output. If, however, they sense unequal fields, they develop unequal voltages, and the output is proportional to the difference in the fields.

The voltage developed by an induction pickup is

$$e = -N \frac{d\phi}{dt} 10^{-8}. \tag{4}$$

For any given device

$$\phi = BA, \tag{5}$$

and

$$\frac{d\phi}{dt} = A \frac{dB}{dt}. \tag{6}$$

Substituting equation (6) into equation (4) gives

$$e = -NA \frac{dB}{dt} 10^{-8}. \tag{7}$$

Since B varies with position, then $\frac{dB}{dt}$ can be replaced by

$$\frac{dB}{dt} = \frac{dB}{dx} \frac{dx}{dt}, \tag{8}$$

and equation (7) becomes

$$e = -NA\ 10^{-8} \frac{dB}{dx} \frac{dx}{dt}. \tag{9}$$

Since $-NA\ 10^{-8}$ is a constant for any given device, equation (9) becomes

$$e = K \frac{dB}{dx} \frac{dx}{dt}. \tag{10}$$

Since $\frac{dx}{dt}$ is velocity, equation (10) becomes

$$e = K \frac{dB}{dx} V. \tag{11}$$

Since $\frac{dB}{dx}$ is the gradient of the flux density, the voltage developed by an inductive sensor is proportional to the gradient of the flux density and to the velocity.

Therefore, there are two major differences in the voltage developed by a Hall device and the voltage developed by an inductive pickup. The Hall device measures the field density directly, independent of velocity, while the inductive pickup measures the gradient of the field density, dependent on velocity.

Both types of sensors may be used to detect the difference of the retained fields of the weld and the base metal.

In order to evaluate these sensors, a disk 18 inches in diameter was cut from one of the weld samples so that the weld formed a diameter of it, and was then mounted on a variable speed drive. The disk was rotated with a maximum surface speed of approximately 600 feet per minute at the sensor. The magnetizer was mounted above the disk with a one-quarter inch air gap between the pole faces of the magnetizer and the surface of the disk. The pole faces were aligned with the center of the disk so that the outer pole was approximately one inch from the edge of the disk.

Six different sensing systems were employed in this evaluation. Two Hall probe arrangements, the single and the differential, were used in the direct measuring methods.

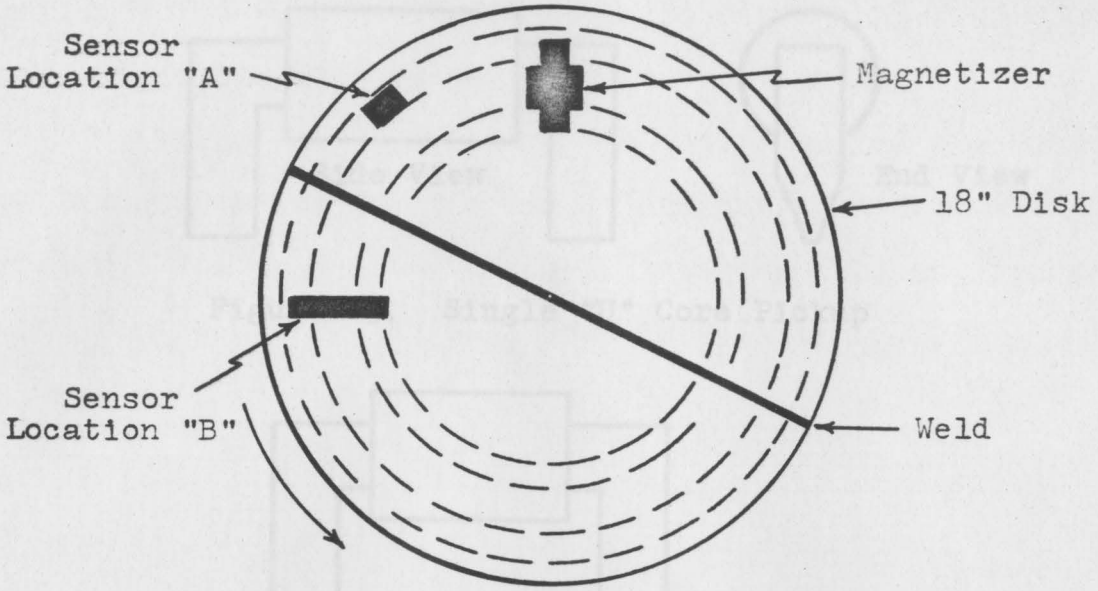

Figure 22. Relative Location of the Magnetizer and the Sensors on the Welded Rotating Disk

Four different inductive pickups were evaluated. These included a tape head, a single "U" core, a double "U" core, and a triangular core. The tape head is the only inductive pickup not specially constructed for this investigation. The other three were constructed, and all these had 200 turns of number 30 AWG enameled wire. The cores were one-quarter inch Ceramag 24A 96-0241 stock. Figures 23, 24, and 25 are sketches of the three specially constructed sensors.

All the sensors except the single "U" core pickup were tested in sensor location "A," shown in Figure 22, and single "U" core was tested in sensor position "B".

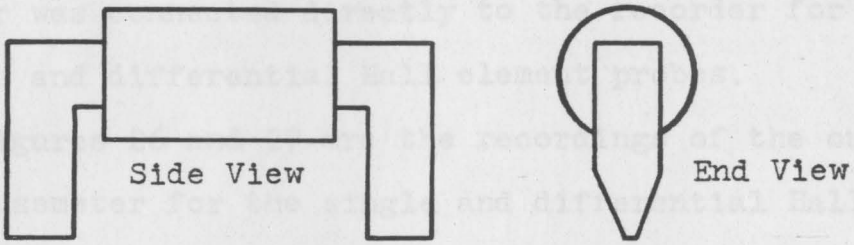

Figure 23. Single "U" Core Pickup

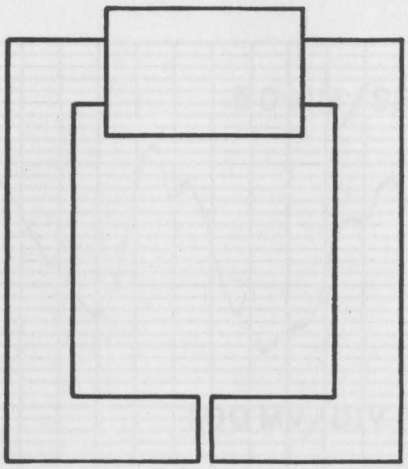

Figure 24. Double "U" Core Pickup

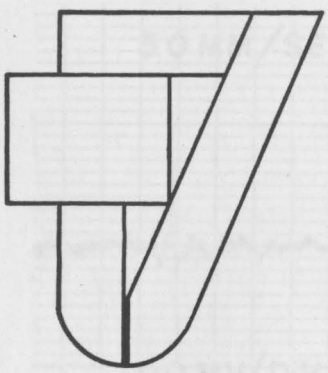

Figure 25. Triangular Core Pickup

All the inductive pickup signals were amplified by an operational amplifier with a gain of 330 and were recorded on a Brush recorder. The output of the Hall

gaussmeter was connected directly to the recorder for both the single and differential Hall element probes.

Figures 26 and 27 are the recordings of the outputs of the gaussmeter for the single and differential Hall probes. The weld area is nearly imperceptible in Figure 26, while in Figure 27 the weld area is well defined.

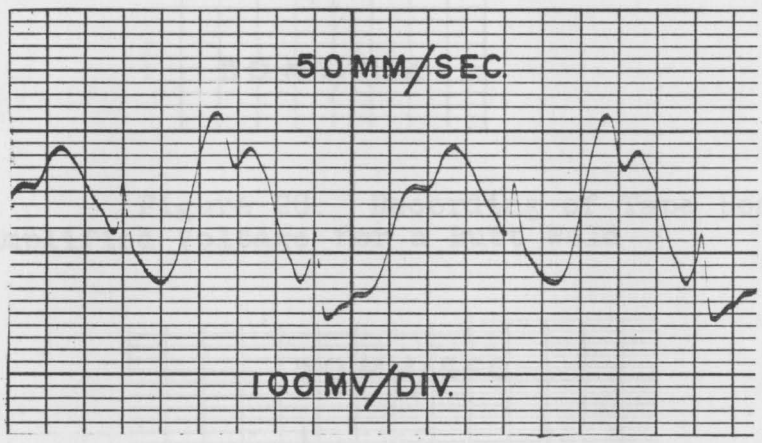

Figure 26. Recording of Single Hall Probe Voltage for a Butt Weld

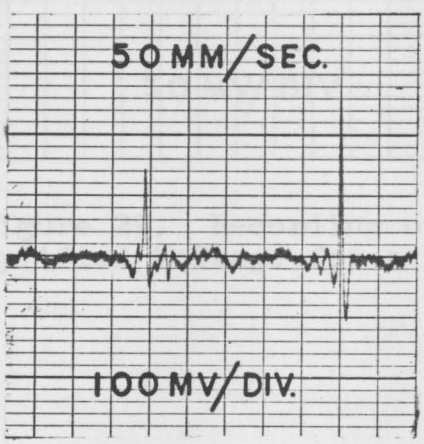

Figure 27. Recording of Differential Hall Probe Voltage for a Butt Weld

Figures 28, 29, 30, and 31 are the recordings of the amplified signals of the four inductive sensors.

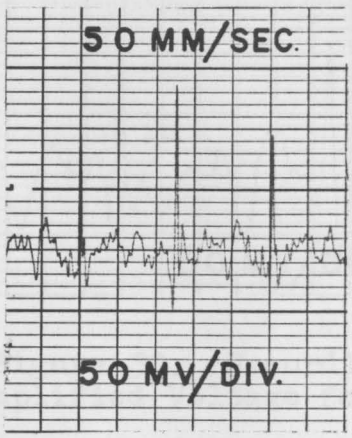

Figure 28. Recording of Tape Head Amplified Voltage for a Butt Weld

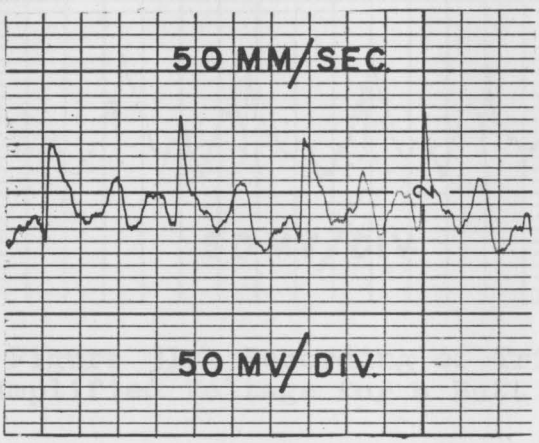

Figure 29. Recording of Single "U" Core Pickup Amplified Voltage for a Butt Weld

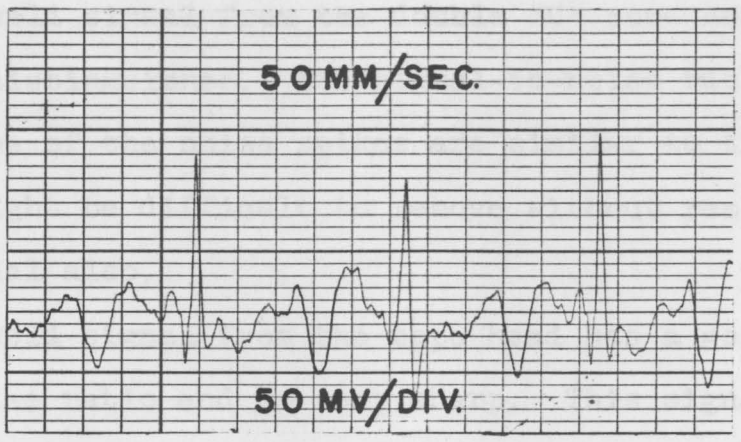

Figure 30. Recording of Double "U" Core Pickup Amplified Voltage for a Butt Weld

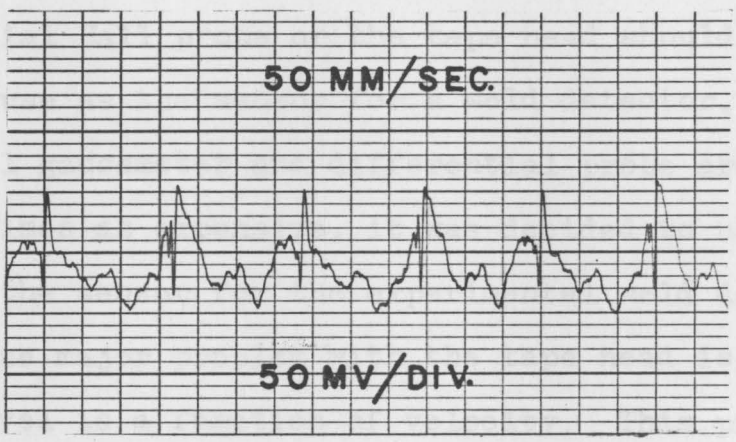

Figure 31. Recording of Triangular Core Pickup Amplified Voltage for a Butt Weld

The weld area is poorly defined in the sensor recordings of the single "U" core and the triangular core. The weld signal from the single "U" core would be very difficult to detect since both the amplitude and duration of the signal are very similar to the noise from the base metal. The weld signal from the triangular sensor might be detectable with proper filtering, since the signal from the weld is sharper than the noise from the base metal.

The weld signal from the double "U" core sensor is more easily distinguished. The signal-to-noise ratio is fair, but some of the noise spikes are similar to the weld signal and might be difficult to remove without removing the weld signal also.

The weld signal from the tape head has a good signal-to-noise ratio and is very sharp. This signal is as good as the weld signal from the differential Hall probe, and superior to the weld signals of all the other sensors.

The tests of different sensors indicate that either the differential Hall probe or the tape head should be suitable for use as the sensor for a weld detector. Since a differential gaussmeter and differential probe are nearly one hundred times as expensive, it was decided to use the tape head as the sensor for the experimental weld detector.

The one major problem with the tape head is that the signal level is a function of velocity. This problem was solved in the design of the experimental weld detector.

CHAPTER III

DESIGN AND CONSTRUCTION OF AN EXPERIMENTAL WELD DETECTOR

In order to design and construct the weld detector, two major problems had to be taken into consideration, since they are commonly found in steel mills. These are strip velocity variations and electrical noise.

In using a narrow bandpass filter to reject electrical noise, it was predicted that the strip velocity would also cause variations in the frequency spectrum of the signal. Therefore, a conventional bandpass filter, tuned for a signal at a given velocity, would attenuate the signal at any other velocity. To substantiate this, the following derivation relates the frequency spectrum of the retained field of the weld to its velocity. The weld area retained field was approximated as shown in Figures 32 and 33. The moving retained field may be approximated in the time domain as shown in Figures 34 and 35. The period T will be dependent on the width of field X and the velocity of the strip V. This relationship is

$$T = \frac{X}{V}. \tag{13}$$

To determine the frequency spectrum the Fourier transform was used since the moving field is an aperiodic function. The Fourier transform is

$$B(JW) = \int_{-\infty}^{\infty} B(t)e^{-JWt}dt. \tag{14}$$

The frequency spectrum for the lap weld was determined with the axis of the simplified flux density shown in Figure 36.

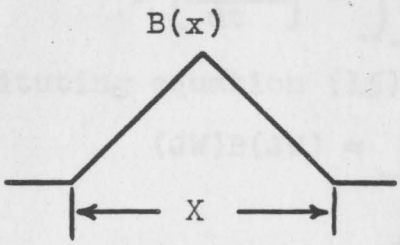

Figure 32. Simplified Retained Field Versus Distance for a Butt Weld

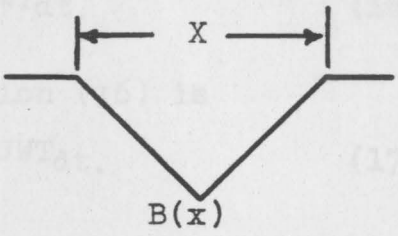

Figure 33. Simplified Retained Field Versus Distance for a Lap Weld

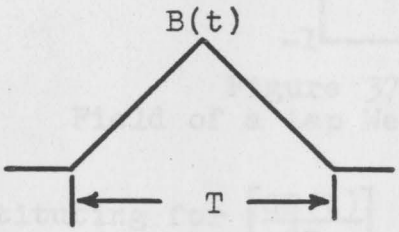

Figure 34. Simplified Retained Field of Period T for a Butt Weld

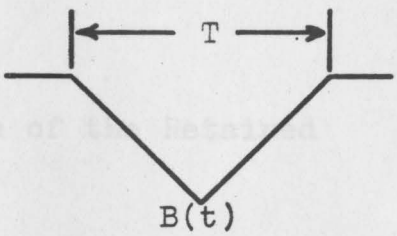

Figure 35. Simplified Retained Field of Period T for a Lap Weld

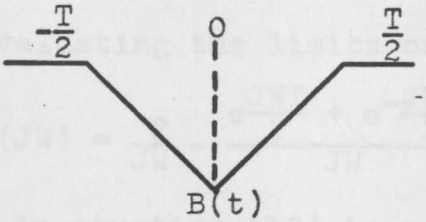

Figure 36. Simplified Retained Field for a Lap Weld

The solution of equation (14) for the function shown in Figure 36 was simplified by using the derivative property. The Fourier transform derivative property is

$$F\left[\frac{d^m B(t)}{dt^m}\right] = (JW)^m B(JW). \qquad (15)$$

The derivative of the moving flux density for a lap weld is shown in Figure 37. The Fourier transform of Figure 37 is

$$F\left[\frac{dB(t)}{dt}\right] = \int_{-\infty}^{\infty}\left[\frac{dB(t)}{dt}\right] e^{-JWT}dt. \tag{16}$$

Substituting equation (15) into equation (16) is

$$(JW)B(JW) = \int_{-\infty}^{\infty}\left[\frac{dB(t)}{dt}\right] e^{-JWT}dt. \tag{17}$$

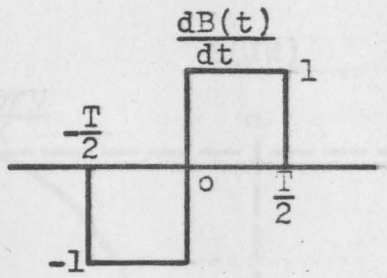

Figure 37. Derivative of the Retained Field of a Lap Weld

Substituting for $\left[\frac{dB(t)}{dt}\right]$ into (17) is

$$(JW)B(JW) = -\int_{-\frac{T}{2}}^{o} e^{-JWT}dt + \int_{o}^{\frac{T}{2}} e^{-JWT}dt. \tag{18}$$

Integrating and evaluating the limits on equation (18) is

$$(JW)B(JW) = \frac{2}{JW} - \frac{e^{\frac{JWT}{2}} + e^{\frac{-JWT}{2}}}{JW} \tag{19}$$

Solving for B(JW) in equation (19) is

$$B(JW) = -\frac{2}{W^2} + \frac{e^{\frac{JWT}{2}} + e^{\frac{-JWT}{2}}}{W^2} \tag{20}$$

To simplify equation (20) the identity

$$\cos X = \frac{e^{JX} + e^{-JX}}{2} \tag{21}$$

was used. Equation (20) then becomes

$$B(JW) = -\frac{2}{W^2} + \frac{2}{W^2}\cos\frac{WT}{2}. \tag{22}$$

Substituting equation (13) into (22) is

$$B(JW) = -\frac{2}{W^2} + \frac{2}{W^2}\cos\frac{WX}{2V}. \qquad (23)$$

B(JW) versus W is plotted in Figure 38. It is evident from Figure 38 that the frequency spectrum is a direct function of velocity.

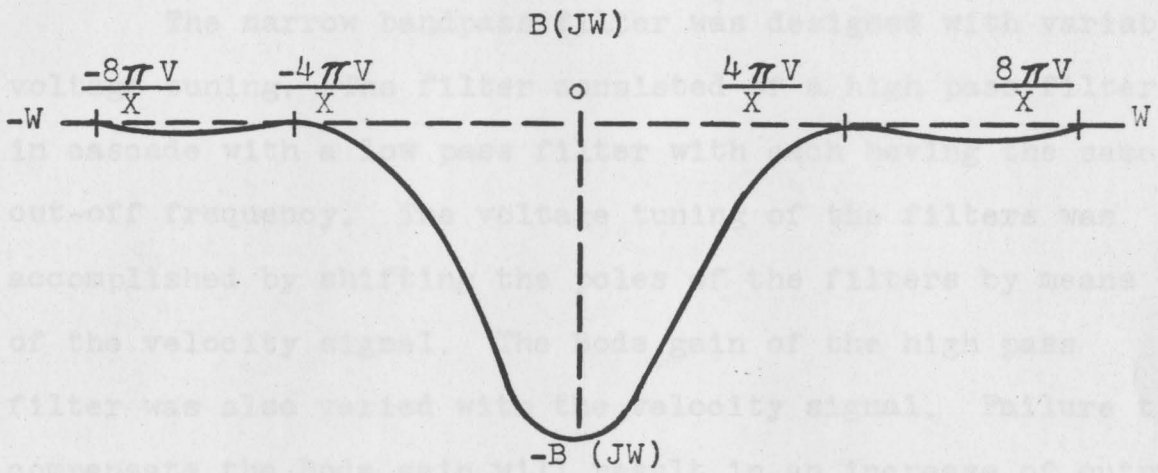

Figure 38. Frequency Spectrum of the Moving Retained Field of a Weld

Therefore, the velocity of the weld affects the inductive sensor signal relative to both amplitude and frequency.

The solution was to design the weld detector circuit to compensate for these problems by making it independent of velocity and insensitive to electrical noise.

The output signal of the inductive sensor was found to be directly proportional to the velocity. This relationship was given in equation (11). Equation (11) is

$$e = K\frac{dB}{dX}V. \qquad (11)$$

If the voltage e is divided by the velocity signal V, the developed voltage e_C is then independent of velocity. This relationship is

$$e_C = \frac{e}{V} = K\frac{dB}{dX}. \tag{24}$$

The voltage e_C of equation (24) is directly proportional to the gradient of the flux density, independent of velocity.

The narrow bandpass filter was designed with variable voltage tuning. The filter consisted of a high pass filter in cascade with a low pass filter with each having the same cut-off frequency. The voltage tuning of the filters was accomplished by shifting the poles of the filters by means of the velocity signal. The Bode gain of the high pass filter was also varied with the velocity signal. Failure to compensate the Bode gain will result in an increase of output of the filter with the increase of the cut-off frequency.

The required transfer function of the high pass filter is

$$G_H(S) = -\frac{\frac{K_1}{V}S}{\frac{K_2}{V}S + 1}. \tag{25}$$

The required transfer function of the low pass filter is

$$G_L(S) = -\frac{K_3}{\frac{K_4}{V}S + 1}. \tag{26}$$

The transfer function of the cascaded filters is

$$G_{BP}(S) = G_H(S)G_L(S). \tag{27}$$

Substituting equations (25) and (26) into (27) is

$$G_{BP}(S) = \left[- \frac{\frac{K_1}{V}S}{\frac{K_2}{V}S + 1} \right] \left[- \frac{K_3}{\frac{K_4}{V}S + 1} \right]. \tag{28}$$

The voltage tuning of the high pass filter was accomplished by the circuit shown in Figure 39. The output voltage of

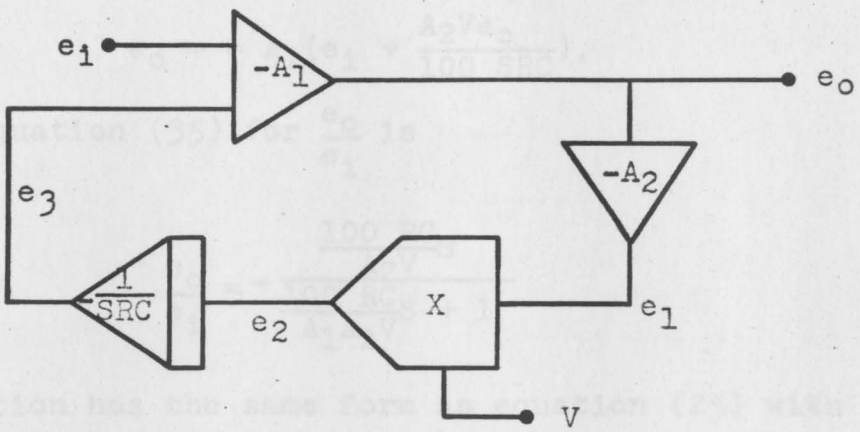

Figure 39. Simplified Circuit Diagram of the High Pass Filter with Variable Voltage Tuning

amplifier A_1 is

$$e_o = - A_1(e_i + e_3). \tag{29}$$

The output voltage of amplifier A_2 is

$$e_1 = - A_2 e_o. \tag{30}$$

The output of the multiplier X is

$$e_2 = \frac{e_1 V}{100}. \tag{31}$$

The output of the integrator is

$$e_3 = - \frac{e_2}{SRC}. \tag{32}$$

Substituting equation (30) into (31) is

$$e_2 = - \frac{A_2 V e_o}{100}. \tag{33}$$

Substituting equation (33) into (32) is

$$e_3 = \frac{A_2 V e_o}{100\ SRC}. \tag{34}$$

Substituting equation (34) into (29) is

$$e_o = - A_1 (e_i + \frac{A_2 V e_o}{100\ SRC}). \tag{35}$$

Solving equation (35) for $\frac{e_o}{e_i}$ is

$$\frac{e_o}{e_i} = - \frac{\frac{100\ RC}{A_2 V} S}{\frac{100\ RC}{A_1 A_2 V} S + 1} \tag{36}$$

This equation has the same form as equation (25) with

$$K_1 = \frac{100\ RC}{A_2} \tag{37}$$

and

$$K_2 = \frac{100\ RC}{A_1 A_2} \tag{38}$$

The simplified circuit diagram of the low pass filter is given in Figure 40. The output of the multiplier X is

$$e_o = \frac{e_1 V}{100}. \tag{39}$$

The output of the integrator is

$$e_1 = - \frac{1}{RCS} (e_o + e_i). \tag{40}$$

Solving for e_1 in equation (39) is

$$e_1 = \frac{e_o 100}{V}. \tag{41}$$

Substituting equation (41) into equation (40) gives

$$\frac{e_o 100}{V} = - \frac{1}{RCS} (e_o + e_i). \tag{42}$$

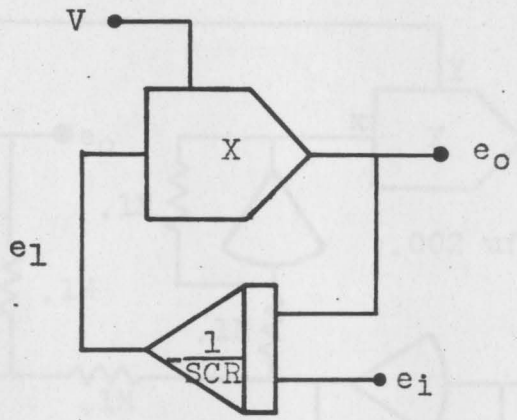

Figure 40. Simplified Circuit Diagram of the Low Pass Filter with Variable Voltage Tuning

Solving for $\frac{e_o}{e_i}$ is

$$\frac{e_o}{e_i} = - \frac{1}{\frac{100\ RC}{V} S + 1}. \tag{43}$$

This equation has the same form as equation (26) with

$$K_3 = 1 \tag{44}$$

and

$$K_4 = 100\ RC. \tag{45}$$

The filter was the first circuitry of the experimental weld detector to be built and tested. The circuitry was patched and tested on two Donner Model 3430 analog computers. The circuit diagram for the voltage tunable bandpass filter is given in Figure 41. The filter was tested by setting the tuning voltage at some level from minus five volts to minus forty volts in five-volt

increments. At each tuning voltage, the input sinusoidal voltage of ten volts RMS was varied in frequency from ten Hertz to 1200 Hertz. The output voltage was recorded for

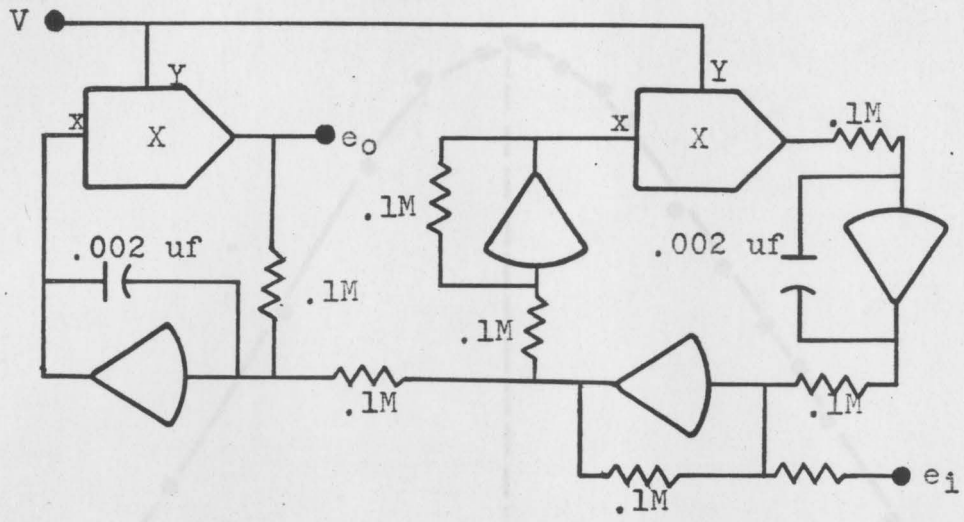

Figure 41. Circuit Diagram of the Voltage Tunable Bandpass Filter

each frequency. Figure 42 is a typical plot of the output voltage amplitude versus frequency for a tuning voltage of minus ten volts.

The frequency of the peak output voltage at each tuning voltage was determined and is shown in Figure 43. From Figure 43 it is apparent that the bandpass frequency is directly proportional to the tuning voltage.

After the filter was designed, built, and tested, the experimental weld detector was then designed. Figure 44 is a block diagram of the experimental weld detector.

The millivolt tape head signal required an amplification of 5000 to be at the proper level. Since the computer amplifiers are very noisy at these large gains, the tape head signal was first amplified by a low noise preamplifier

with a gain of 250. This amplified signal was then further amplified by a computer amplifier with a gain of 20. This method of amplification produced a comparatively noise-free signal.

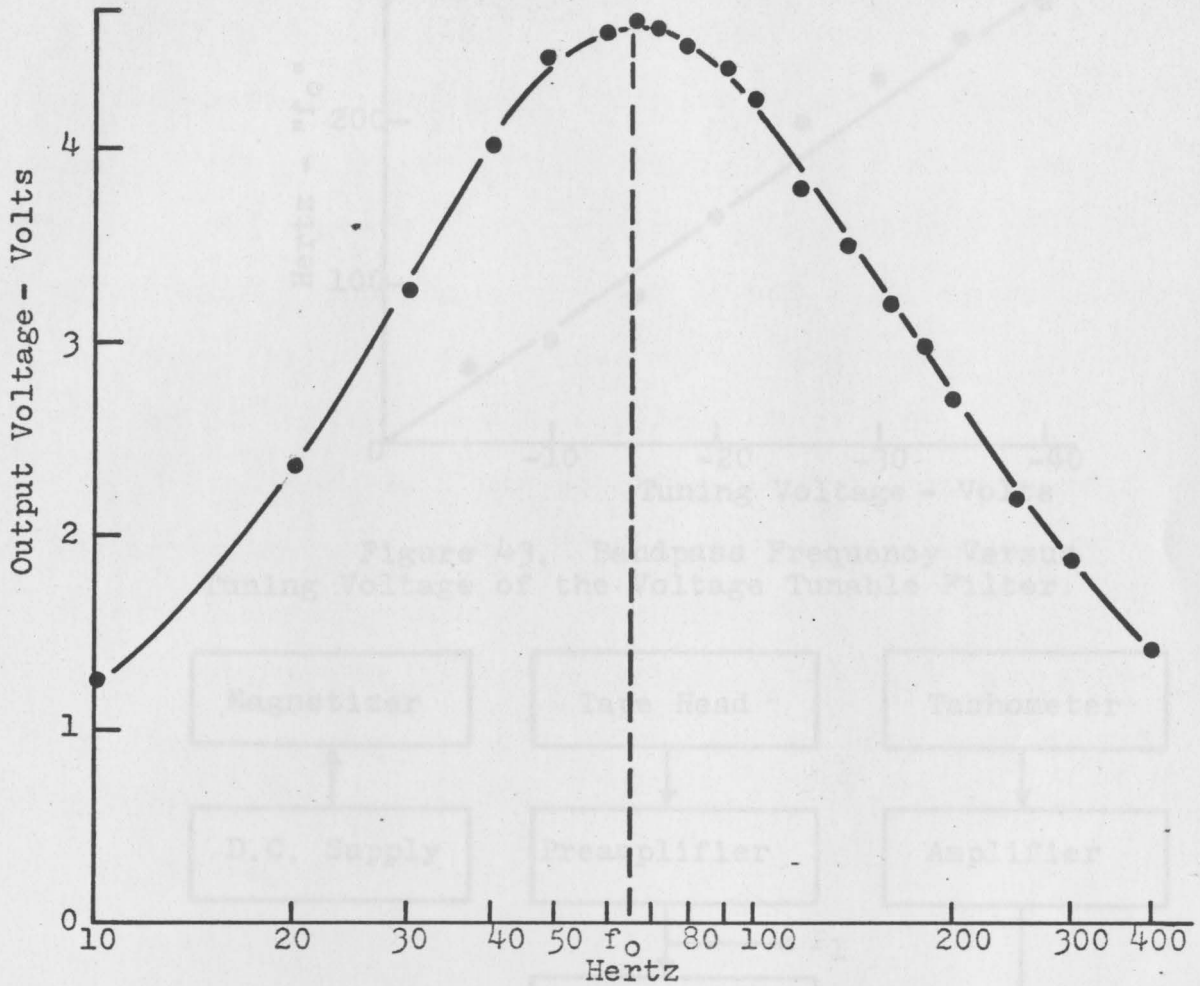

Figure 42. Plot of the Output Voltage Versus Frequency of the Bandpass Filter with a Tuning Voltage of Minus Ten Volts

The welded eighteen-inch disk was used in the experimental system. The tachometer was connected to the disk by means of a rubber wheel connected to the shaft of the tachometer with the wheel riding on the outer edge of the surface of the disk.

The signals at different locations in the weld detector circuitry were recorded on a six-channel Brush recorder. The signal locations are shown in Figure 44.

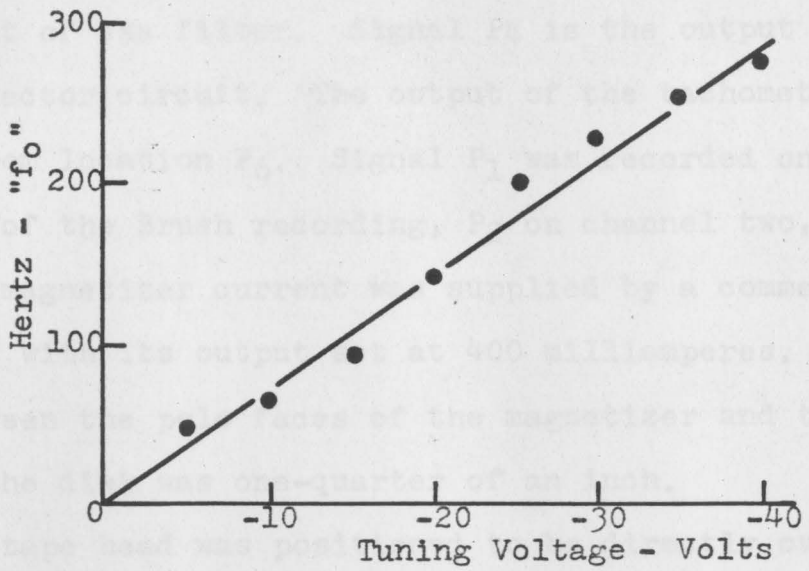

Figure 43. Bandpass Frequency Versus Tuning Voltage of the Voltage Tunable Filter.

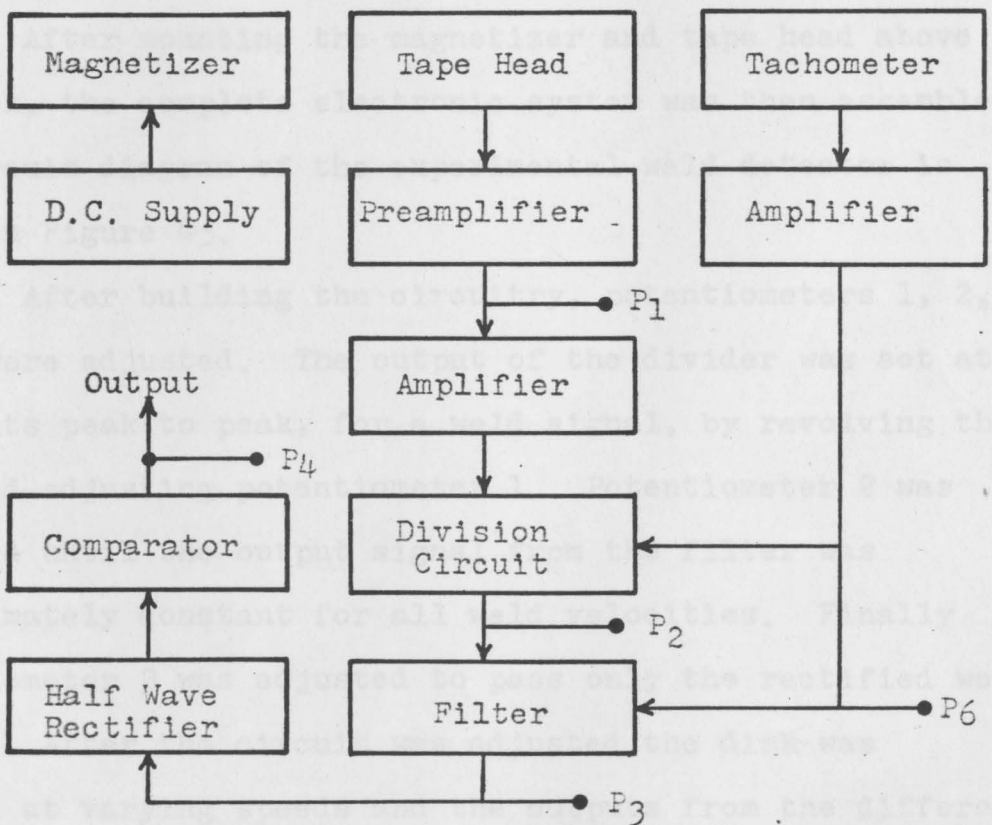

Figure 44. Block Diagram of the Experimental Weld Detector

Signal location P_1 is the amplified output of the tape head. Signal location P_2 is the output of the amplified tape head signal divided by the velocity signal. Signal P_3 is the output of the filter. Signal P_4 is the output of the weld detector circuit. The output of the tachometer was taken from location P_6. Signal P_1 was recorded on channel one of the Brush recording, P_2 on channel two, etc.

The magnetizer current was supplied by a commercial power supply with its output set at 400 milliamperes. The air gap between the pole faces of the magnetizer and the surface of the disk was one-quarter of an inch.

The tape head was positioned to be directly over the inner magnetized pole of the disk. The air gap of the tape head was also set at one-quarter of an inch.

After mounting the magnetizer and tape head above the disk, the complete electronic system was then assembled. The circuit diagram of the experimental weld detector is given in Figure 45.

After building the circuitry, potentiometers 1, 2, and 3 were adjusted. The output of the divider was set at ten volts peak to peak, for a weld signal, by revolving the disk and adjusting potentiometer 1. Potentiometer 2 was adjusted until the output signal from the filter was approximately constant for all weld velocities. Finally potentiometer 3 was adjusted to pass only the rectified weld signal. After the circuit was adjusted the disk was rotated at varying speeds and the outputs from the different

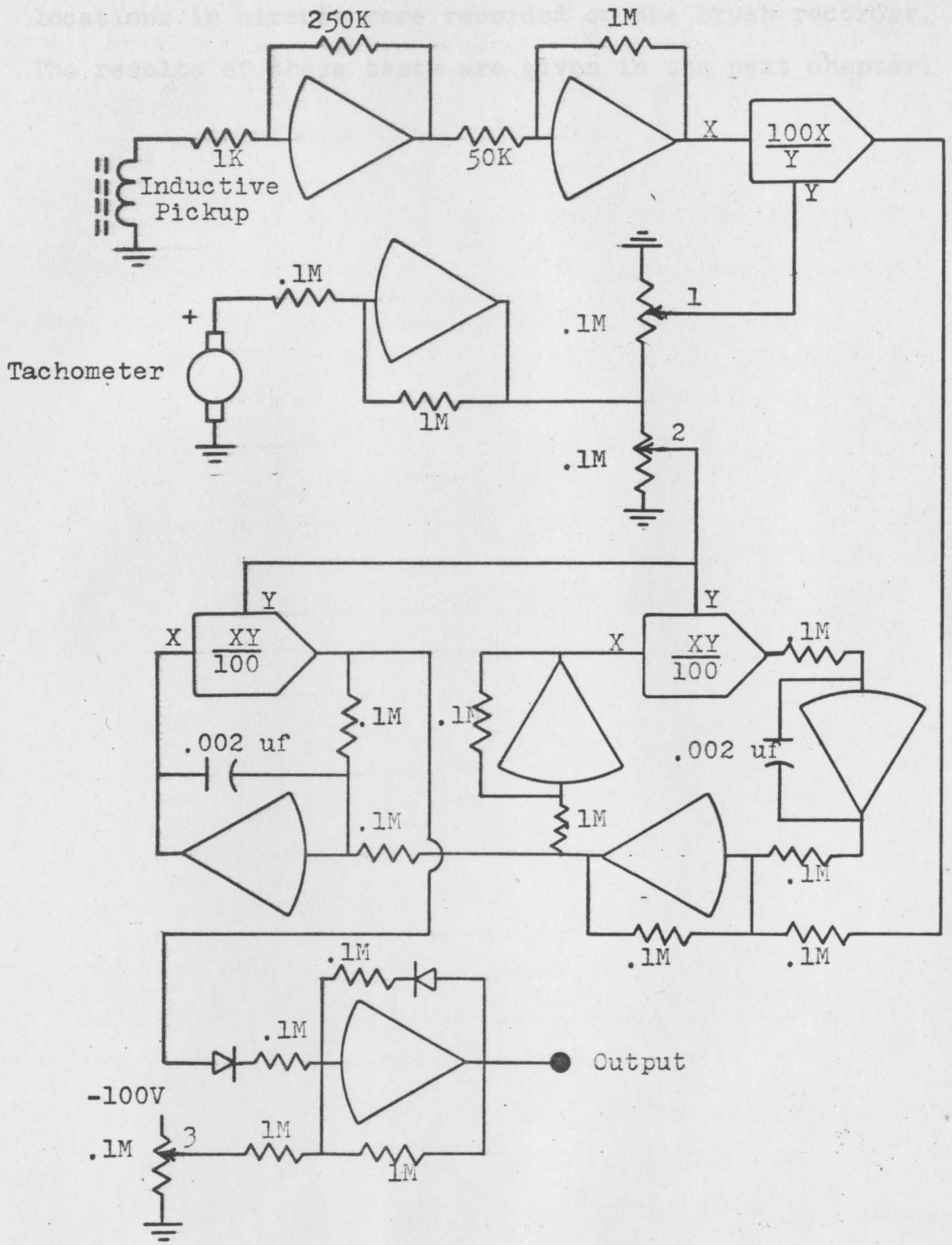

Figure 45. Circuit Diagram of the Experimental Weld Detector

locations in circuit were recorded on the Brush recorder. The results of these tests are given in the next chapter.

CHAPTER IV

WELD DETECTOR TEST RESULTS, CONCLUSIONS, AND RECOMMENDATIONS

The output of the tape head was directly proportional to the velocity of the weld. The plot of the amplified tape head signal versus velocity is given in Figure 46.

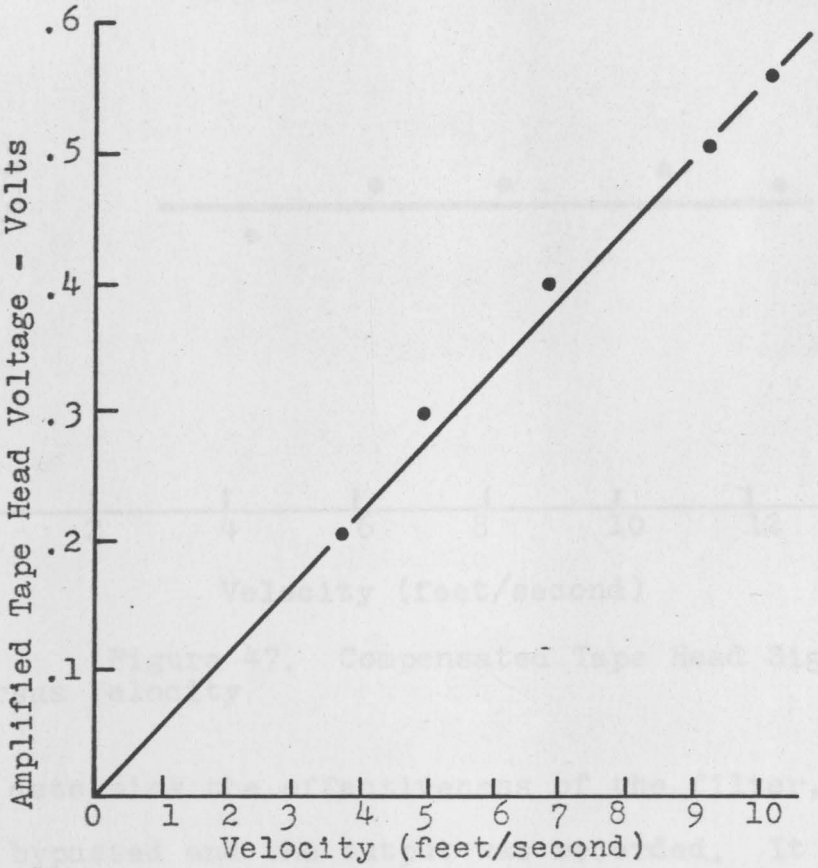

Figure 46. Amplified Tape Head Signal Versus Velocity

These changes in amplitude of the tape head signal with changes in velocity were compensated for by the circuitry very well. It is apparent from Figure 47 that the output from the division circuit is constant over the full range of velocity tested.

Figure 48 is a typical recording of the different signals of the detector. It may be noted that the output signal is very sharp with very little noise.

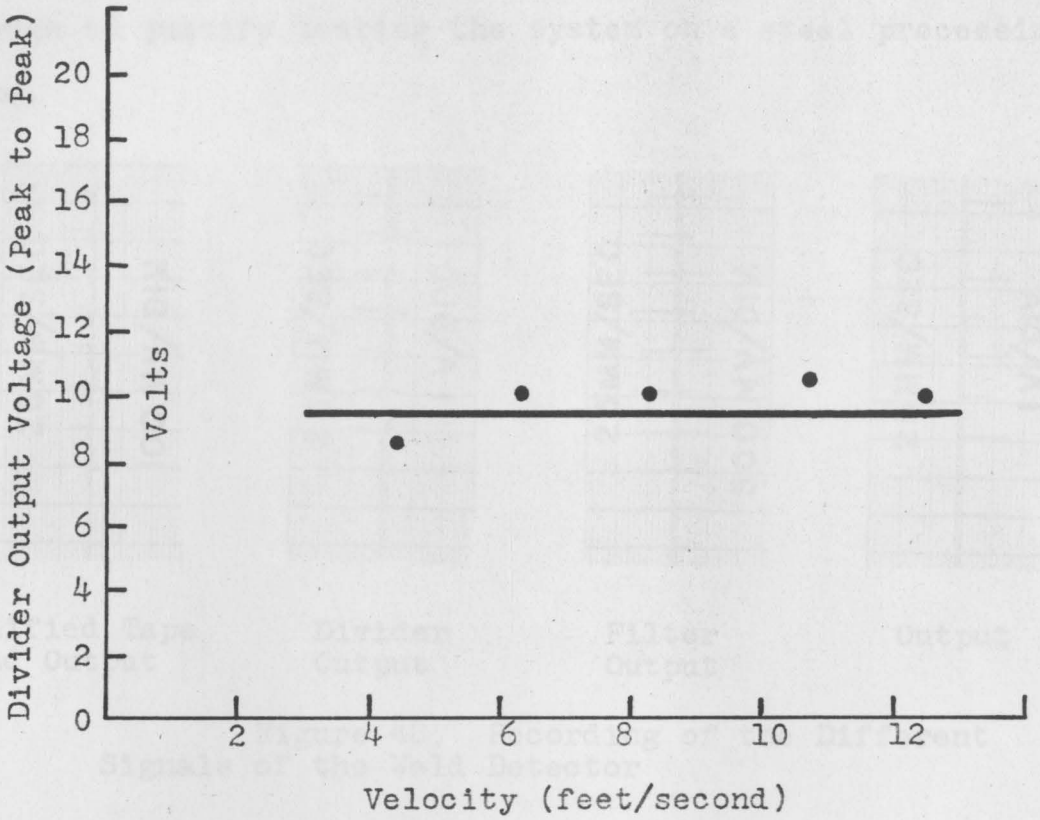

Figure 47. Compensated Tape Head Signal Versus Velocity

To determine the effectiveness of the filter, the filter was bypassed and the output was recorded. It is evident that the noise level is higher without the filter.

One possible improvement in the system would be to use a full wave rectifier in place of the half wave rectifier. Often the weld signal has a large peak in one direction and a small peak in the other direction. A full

wave rectifier would insure the largest peak would not be clipped.

In view of the results of all the tests on the experimental weld detector, the tests were encouraging enough to justify testing the system on a steel processing line.

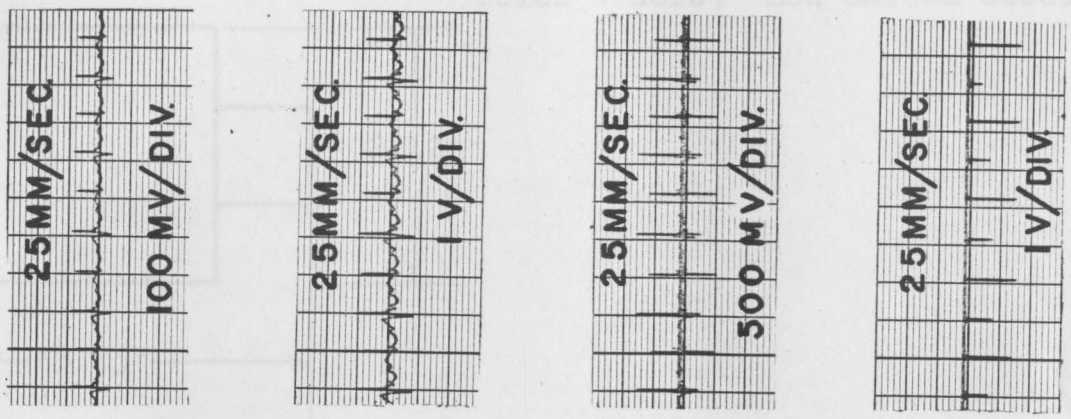

Amplified Tape Head Output | Divider Output | Filter Output | Output

Figure 48. Recording of the Different Signals of the Weld Detector

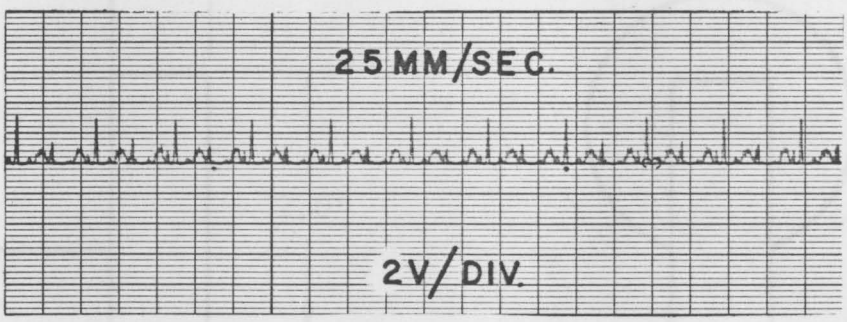

Figure 49. Recording of the Output of the Weld Detector without the Filter

APPENDIX

Coil Resistance = 22.5 Ω
Wire Size = #24AWG
Coil Turns = 2200
Poles + Core: Low Carbon Steel

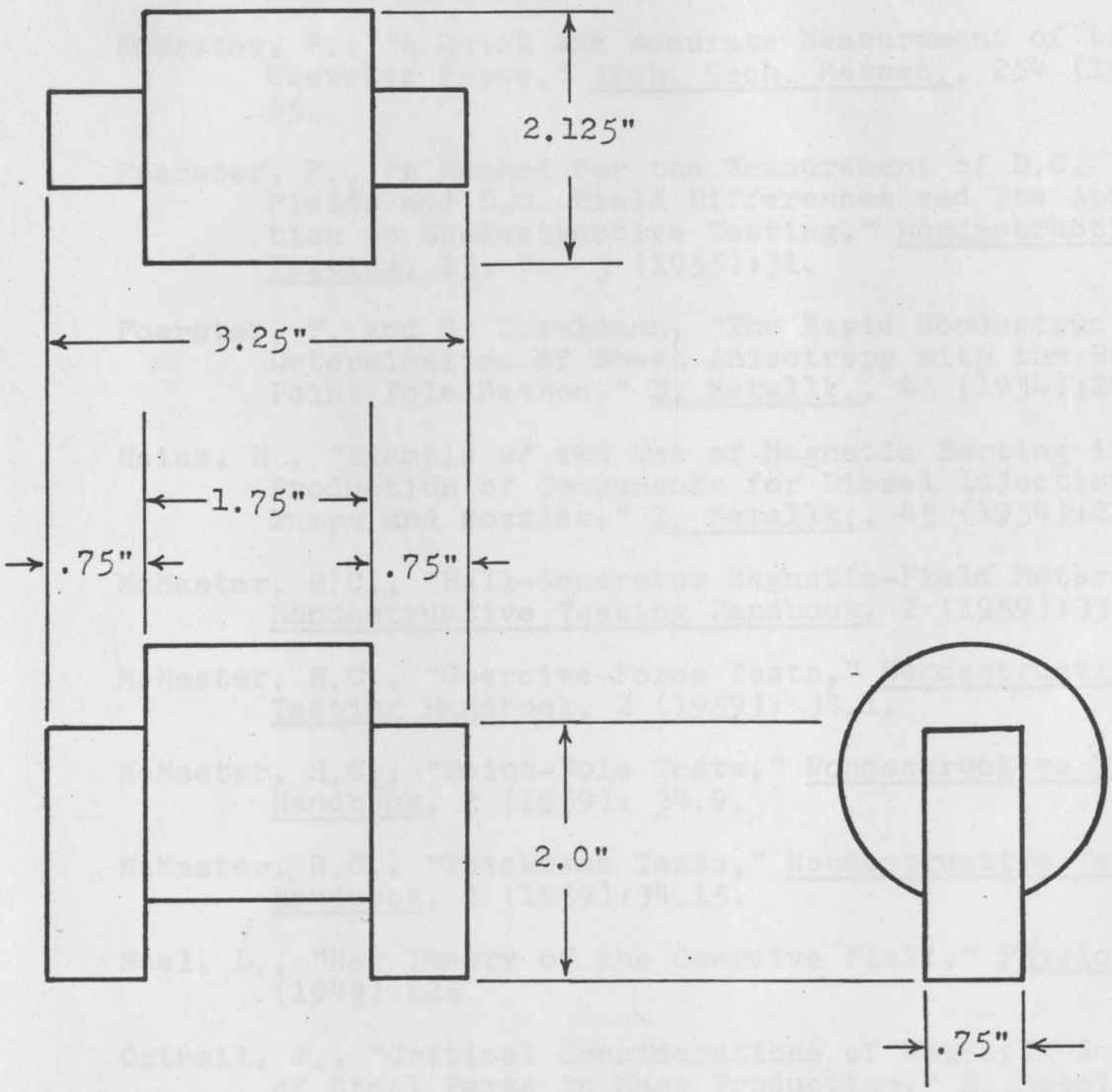

Figure 13. Magnetizer

REFERENCES

Borowik, A., "Ferromagnetic Metals Identification and Measurement of Internal Stresses, Part 1, Magnetic Tests," Iron and Steel, 21 (1948): 3,39.

Brown, R.J. and J.H. Bridle, "A New Method of Sorting Steels," Engineer, 176 (1943):442.

Faulkner, W.H. Jr. and J.G. Wood, "Thickness Measurement of Sheet and Web Materials," Handbook of Applied Instrumentation (1964):6-16.

Foerster, F., "A Quick and Accurate Measurement of the Coercive Force," Arch. Tech. Messen., 254 (1957): 65.

Foerster, F., "A Method for the Measurement of D.C. Fields and D.C. Field Differences and Its Application to Nondestructive Testing," Nondestructive Testing, 13, No. 5 (1955):31.

Foerster, F. and G. Zizelmann, "The Rapid Nondestructive Determination of Sheet Anisotropy with the Residual Point Pole Method," Z. Metallk., 45 (1954):245.

Hainz, R., "Example of the Use of Magnetic Sorting in the Production of Components for Diesel Injection Pumps and Nozzles," Z. Metallk., 45 (1954):238.

McMaster, R.C., "Hall-Generator Magnetic-Field Meters," Nondestructive Testing Handbook, 2 (1959):33.11.

McMaster, R.C., "Coercive-Force Tests," Nondestructive Testing Handbook, 2 (1959): 34.1.

McMaster, R.C., "Point-Pole Tests," Nondestructive Testing Handbook, 2 (1959): 34.9.

McMaster, R.C., "Thickness Tests," Nondestructive Testing Handbook, 2 (1959):34.15.

Neel, L., "New Theory of the Coercive Field," Physica, 15 (1949):225.

Ortheil, J., "Critical Considerations of Magnetic Sorting of Steel Parts in Mass Production," Z. Metallk., 45 (1954):243.

REFERENCES (CONT.)

Schneider, P.H. and P. Dekker, "The Measurement of Wall Thickness with the Foerster Kawimeter," Metall., 3 (1949):321.

Underhill, E.M., Permanent Magnet Design (Pittsburgh, Pa.: Crucible Steel Company of America, 1957), p. 2-23.

_____, "Method for Measuring Steel Hardness," British Patent 1,186,692.